Published in final edited form as:
Acta Biomater. 2015 February ; 13: 111–120. doi:10.1016/j.actbio.2014.10.039.

Electrospun fiber constructs for vocal fold tissue engineering: effects of alignment and elastomeric polypeptide coating

Lindsay A. Hughes, M.A.Sc,
Department of Chemical Engineering, Queen's University, 201 Dupuis Hall, 19 Division Street, Kingston, ON K7L 3N6

Joel Gaston, BS,
Department of Surgery and Biomedical Engineering, University of Wisconsin –Madison, 5118 WIMR, 1111 Highland Ave, Madison, WI 53705

Katherine McAlindon, M.A.Sc,
Department of Chemical Engineering, Queen's University, 201 Dupuis Hall, 19 Division Street, Kingston, ON K7L 3N6

Kimberly A. Woodhouse, PhD, and
Professor, Department of Chemical Engineering, Queen's University, 201 Dupuis Hall, 19 Division St, Kingston, ON K7L 3N6

Susan L. Thibeault, PhD
Associate Professor, Departments of Surgery, Biomedical Engineering and Communication Sciences and Disorders, University of Wisconsin Madison, 5107 WIMR, 1111 Highland Ave, Madison, WI 53705

Abstract

Vocal fold lamina propria extracellular matrix (ECM) is highly aligned and when injured, becomes disorganized with loss of the tissue's critical biomechanical properties. This study examines the effects of electrospun fiber scaffold architecture and elastin-like polypeptide (ELP4) coating on human vocal fold fibroblast (HVFF) behavior for applications toward tissue engineering the vocal fold lamina propria. Electrospun Tecoflex™ scaffolds were made with aligned and unaligned fibers, and were characterized using scanning electron microscopy and uniaxial tensile testing. ELP4 was successfully adsorbed onto the scaffolds; HVFF were seeded and their viability, proliferation, morphology, and gene expression were characterized. Aligned and unaligned scaffolds had initial elastic moduli of ~14 MPa, ~5 MPa and ~0.3 MPa, ~0.6 MPa in the preferred and cross-preferred directions, respectively. Scaffold topography had an effect on the orientation of the cells, with HVFF seeded on aligned scaffolds having a significantly different ($p < 0.001$) angle of orientation than HVFF cultured on unaligned scaffolds. This same effect and

Correspondence to: Susan L. Thibeault.

significant difference ($p < 0.001$) was seen on aligned and unaligned scaffolds coated with ELP4. Scaffold alignment and ELP4 coating impacted ECM gene expression. ELP4 coating, and aligned scaffolds upregulated elastin synthesis when tested on day 7 without a concomitant upregulation of collagen III synthesis. Collectively, results indicate that aligned electrospun scaffolds and ELP4 coating, are promising candidates in the development of biodegradeable vocal fold lamina propria constructs.

Keywords

electrospinning; elastin; vocal folds; fibroblasts; alignment; gene expression

1. Introduction

Voice disorders affect up to 9% of the population at any time, resulting in hoarseness or complete voice loss[1] and can be caused by misuse, hyperfunction, medical conditions, or as a result of surgery[2]. The response of the vocal fold to an injury can cause scar tissue, changing the organization and composition of the vocal fold lamina propria, altering the biomechanical properties of the tissue and subsequent production of mucosal wave resulting in abnormal voice quality[2]. At the present time, there are few treatment options for vocal fold scarring and research utilizing tissue engineering strategies to design effective treatments for vocal fold scarring have included growth factor therapies, cell therapies and biomaterials[3–9]. Biomaterials, aim to be biocompatible, biodegradable, improve matrix production, reduce scar tissue, as well as have biomechanical properties that closely mimic native vocal fold tissue.

Electrospinning, a versatile technique, produces nano to microfibers by applying electrical fields to an ejected polymer solution. Electrospun biomaterials provide a structural network for the cells to grow on during repair and regeneration. The topographic alignment of nanofibers has been demonstrated to influence cell orientation in the fiber direction, morphology and proliferation. Moreover, because many of the body's tissues, including the vocal fold, have aligned structured ECM networks, the ability for electrospinning to produce scaffolds with highly aligned fiber formations is being widely utilized[10]. Fiber alignment, and pretreating scaffolds with fibroblast cells improve embryonic stem cell-derived cardiomyocytes differentiation indicating that fiber alignment may be an important parameter for engineering myocardial tissue[11]. Further, higher fibroblast cell adhesion has been shown to be greater on randomly aligned electospun collagen scaffolds than aligned scaffold after seven hours, however there was greater proliferation on the aligned scaffold over a seven-day period; morphology also followed the alignment of the fibers[12]. Fiber alignment of scaffolds has been shown to affect gene expression, and morphology of Schwann cells[13], as well as morphology and proliferation of fibroblast cells and smooth muscle cells[12, 14]. Due to the highly aligned and organized nature of the vocal fold lamina propria[15], growth on an aligned scaffold may affect the morphology and gene expression of vocal fold fibroblasts in turn promoting matrix synthesis and matrix organization improving healing, and resulting in improved biomechanical properties of the tissue.

Elastin protein makes up around 9% of the total protein component in the vocal fold lamina propria, which is greater than that of skin, but less than that of the lungs and arteries[16]. Elastin protein is typically only produced during the pre- and neonatal stages of development, with fibroblasts secreting minimal amounts during adult years[17]. The structure of elastin needs to support numerous expansions and recoil for tissue function, and as such elastin fibers are often combined with collagen fibers to regulate stretching and to prevent tissue damage[16]. In healthy vocal folds, elastin is organized in long, somewhat parallel fibers with collagens whereas elastin fibers in scarred vocal folds are disorganized and collagen bundles are dense and thick, while the elastin fibers are sparse[18, 19]. Elastin-like polypeptides (ELPs) derived from the elastin gene and produced using recombinant methods have been shown to have similar properties to native elastin, including the ability to self-assemble[20, 21] and can be modified to contain specific amino acid sequences for the desired functionality. A family of ELPs has been purified, expressed, and designed to contain alternating crosslinking domains and hydrophobic domains similar to those of tropoelastin[20, 21]. Specifically, ELP4 has a 20-24-24-24-24 gene sequence, with the crosslinking domains 21 and 23 between the hydrophobic domains. The sequencing in exon 24 contains the repeating sequence VGVAPG.

Introducing elastin as a coating on biomaterials could provide cell signaling for improved cell growth and regeneration. ELPs have been investigated as a coating for vascular applications, reducing platelet activation, and thrombogenicity on synthetic materials *in vitro*[22, 23] and as elastin coatings on poly(glycerol sebacate) scaffolds, which have been shown to promote endothelial progenitor cell adhesion and proliferation[24]. Human skin fibroblasts have an elastin receptor, a 67 kDa glycoprotein, and elastin derived polypeptides (EDPs) coated on petri dishes, or added to media promote cell growth[25]. Further, EDPs promote MMP-2, which degrades collagen type IV and has some elastinolytic ability[26]. Such activity could aid in tissue remodeling of disorganized elastin and collagen fibers evident in vocal fold scar tissue.

Despite the potential uses of nanofibers for vocal fold tissue engineering applications, little information is available on the influence of aligned and unaligned constructs on cell behavior, as well as the addition of an elastin coating on these nanofibers, for a soft tissue whose biomechanical properties are vital for function. The aim of this study is to use an elastomeric electrospun biomaterial seeded with vocal fold fibroblasts as an in vitro model system to evaluate morphology, viability, proliferation and gene expression in response to material architecture (aligned and unaligned) with and without an elastin polypeptide (ELP) surface coating. Results will guide the future development of constructs for vocal fold tissue engineering.

2. Materials and Methods

All chemicals were from Sigma-Aldrich, St. Louis, MO unless otherwise stated.

2.1. Electrospinning Tecoflex™ Scaffolds

Tecoflex™ SG-80A beads, (Thermedics, Wickliffe, OH) were first dissolved in chloroform (3% w/v), then filtered through Whatman 40 paper, and cast into a mold that was placed in a

vacuum oven overnight then stored in a desiccator until use. In preparation for electrospinning, solutions of 10% w/v concentration were made by dissolving the mold in dichloromethane (DCM) (Fisher Scientific, Ottawa, ON). Electrospun scaffolds were made using a 10 w/v% solution and loaded into a 5 mL plastic syringe (Becton Dickenson, Franklin Lakes, NJ) with a 1″ 22 gauge blunt end needle (Kontes Glass Company, Vineland, NJ) and placed on a syringe pump (KD Scientific, Holliston, MA) running at 1 mL/hour. Electrospinning was carried out under ambient conditions in a ventilated area on a custom-made electrospinning apparatus. The grounded collection mandrel was positioned at a distance of 25 cm from the needle tip. A high power voltage supply (Gamma High Voltage Research Inc, Ormond Beach, FL) applied a voltage of 15 kV to the needle tip. To make the aligned scaffold, the mandrel was set at a translation speed of 3 m/s and a rotation of 410 cm/s. To make the unaligned scaffold, the mandrel was set at a translation speed of 3 m/s and a rotation of 5 cm/s. Scaffolds were made to a thickness of approximately 50 – 80 μm (~45 h), measured by a caliper. Completed scaffolds were left on the mandrel for two days to ensure solvent removal, and then placed in a desiccator until use.

2.2. Scaffold Characterization

Scaffolds were characterized by imaging with a scanning electron microscope (SEM). Discs of the scaffold were punched out using a 6 mm biopsy punch, and placed on metal stubs using carbon tape. Punches were gold coated for ten minutes on a pulse setting. Images were taken using an SEM (Model Jeol JSM-840, Queen's University, Mechanical and Materials Engineering Department) with an accelerating voltage of 10 kV. Using ImagePro Premier the fiber diameters and angles for the aligned and unaligned scaffolds were measured manually from 300 fibers using a random dot generator from at least 3 different images taken for each scaffold type. In order to determine pore sizes for each condition, SEM images were analyzed in Adobe Photoshop. Using the scale bar the number of pixels corresponding to 1 μm was determined for each pore.

2.3. Mechanical Properties

Mechanical properties of the scaffolds were determined using uniaxial testing, and testing was performed under ASTM D1708. Scaffolds were preconditioned at ~24°C and 55% humidity for 48 hours. Aligned and unaligned samples were tested in the preferred and cross-preferred directions, with preferred being parallel to the mandrel rotation, and cross-preferred being perpendicular to the mandrel rotation. At least 5 samples were tested for each condition at a size of 1 cm wide and 2 cm long. To make handling of the samples easier for testing, paper windows were cut with an inner length of 1.5 cm. A strip of double-sided tape was placed on the top and bottom of the windows and scaffold pieces were placed lengthwise on top. Samples were then placed in the grips so that the gauge length was the 1.5 cm window length. Testing was done using a Mach-1 device (Human Mobility Research Center, Queen's University) with a 10 N load cell, and a crosshead speed of 9 mm/min. Samples were stretched until failure or the maximum displacement of the machine. The cross sectional area of the scaffolds were estimated using the mass of the sample, the density of the polymer, and average fiber diameter to determine the number of fibers and in turn the cross sectional area of all fibers[27]. Initial modulus was calculated from the stress-strain

graphs, and statistical analysis was performed using one-way ANOVA with Bonferroni post hoc analysis.

2.4. Elastin Polypeptide Coating

A Fastin™ Elastin (Biocolor, Carrickfergus, UK) assay was performed to determine the amount of ELP4 absorbed to the surface on three replicates from three samples. Aligned and unaligned samples cut with 6 mm biopsy were prepared by an overnight equilibration in PBS as well as an overnight coating in 50 μg/mL fibronectin solution. Samples were coated in ELP4 for one hour as described above, and then the assay was performed. Microcentrifuge tubes were prepared in duplicates for a reagent blank of 100 μL of the ELP4 solution, standards for 12.5, 25, and 50 μg of ELP4, and 100 μL of the test samples. An equal volume of the Elastin Precipitating Reagent was added to each tube, vortexed, and left to stand for 15 minutes. Tubes were then centrifuged at 10,000 × g for 10 minutes, and liquid was removed. To each tube, 1 mL of Dye Reagent was added, tubes were then vortexed and left to stand for 1.5 hours, followed by a centrifugation step at 10,000 × g for 10 minutes. Liquid in the tubes was then removed and a Q-tip was used to remove any excess fluid in the top half of the tubes. Finally, 250 μL of Dye Dissociation reagent was added to each tube, vortexed, and vortexed again after 10 minutes. Samples were then put into a 96 well plate, and read in a micro plate reader at a wavelength of 513 nm.

2.5. Human Vocal Fold Fibroblast Culture and Seeding onto Tecoflex® Scaffolds

Immortalized human vocal fold fibroblasts (HVFF)[28] were grown on tissue culture polystyrene flasks in a media composed of Dulbecco's Modified Eagle's Medium (DMEM), 1% penicillin/streptomycin, 1% MEM-non-essential amino acids, and 10% fetal bovine serum (FBS). Medium was changed every other day, and the cells were split when they reach ~80% confluence. Scaffolds were punched out using a 6 mm biopsy punch, subsequently disinfected with 250 uL of 70% ethanol for 20 minutes and UV light for 20 minutes and equilibrated in 250 uL of phosphate buffered saline solution (PBS) (Thermo Scientific, Ottawa, ON) overnight at 37°C in 96 non-tissue culture treated 96 well plates. Scaffolds were coated in fibronectin with 100 uL of 50 μg/mL solution overnight at 37°C. On the day of seeding, half of the samples were statically coated with 100 uL of a 1 mg/mL ELP4 solution in 70% ethanol for one hour. ELP4 surface concentration was determined based on previous work[29]. Cells, from passage 6–10, were statically seeded on one side of the scaffold at a cell density of 50,000 cells/scaffold in non-tissue culture treated 96 well polystyrene plates. Every day 75% of the media was changed. Scaffolds were characterized over days 1, 3 and 7. For gene expression scaffolds were equilibrated with 2 mL of PBS, coated in 1 mL of the fibronectin solution, and coated in 1 mL of the ELP4 solution. Seeding density was 500,000 cells/scaffold and scaffolds were cultured in non-tissue culture treated 6 well plates.

2.6. HVFF Viability and Proliferation

Viability and proliferation of the seeded Tecoflex® scaffolds were determined during the culture period using Live/Dead® staining and PicoGreen® and alamarBlue® assays. A Live/Dead® (Invitrogen, Carlsbad, CA) assay was used to ascertain whether cells were living or dead on the scaffolds on days 3 and 7. Three samples in three separate trials were stained

with 200 uL of calcein AM and ethidium homodimer-1 at concentrations of 4 μM and 20 μM in PBS respectively for 35 minutes at room temperature (RT). Results were examined with an Olympus IX81 FV1000 confocal microscope at the Human Mobility Resource Center (HMRC; Kingston General Hospital, Kingston, ON) using excitation/emission spectrum of 495/515 and 495/635 for calcein and ethidium homodimer-1 respectively.

Cell proliferation was assessed with alamarBlue® and PicoGreen® (Invitrogen, Carlsbad, CA). Samples for both tests were seeded at the same time, and tests were run on days 1, 3, and 7. The tests were run three separate times with six duplicate samples each time (n=6, N=3). The alamarBlue assay was run per manufacturer's instructions with an incubation time of three hours. Duplicates of each well were made, with a total assay volume of 100 uL per well. The plate was read in a PerkinElmer 2300 Enspire™ Mutimode Plate Reader (Human Mobility Research Center, Queen's University). For the PicoGreen® assay, media was removed from the wells and the scaffolds were washed once with PBS for three replicates from three samples. Samples were then subjected to three freeze/thaw cycles at −80°C. The PicoGreen assay was then run on the samples according to the manufacturer's instructions. Fluorescence was read at excitation and emission wavelengths of 480/520 nm.

2.7. HVFF Morphology

Matrix deposition was determined using immunostaining for alpha-smooth muscle actin (α-SMA), collagen-1, and 4′,6-diamidino-2-phenylindole (DAPI) as previously used by the Thibeault lab [30–33]. Briefly, samples were washed with PBS and fixed in 4% paraformaldehyde in PBS for 30 minutes at RT. Fixed scaffolds were washed 3 times in blocking solution of 2% bovine serum albumin (BSA), 3% FBS in PBS. 100 uL of a permeabilization reagent (Invitrogen, Carlsbad, CA), was added for 10 minutes at RT; cells were washed again with fresh blocking solution 3 times and incubated at RT in 100 uL of mouse monoclonal anti-alpha smooth muscle actin and rabbit monoclonal anti-collagen 1 (Abcam®, Toronto, ON), both at a dilution of 1:200 and 1:500, respectively, in PBS with 5% blocking solution, for one hour. Goat anti-mouse IgG1 (Invitrogen, Carlsbad, CA) and goat anti-rabbit (Invitrogen, Carlsbad, CA), 100 uL solutions at a dilution of 1:1000 in blocking solution were added for one hour. Scaffolds were labeled with 100 uL of DAPI at 0.5 μg/mL in PBS for 10 minutes and were washed 3 times with blocking solution between each step. Stains were viewed using a confocal microscope using excitation/emission wavelengths of 358/461 nm for DAPI and 495/519 nm for α-SMA and 579/603 nm for collagen-1.

Cell morphology was viewed by using an actin cytoskeleton staining kit (Chemicon® International, Temecula, California). Nuclei, focal adhesions, and actin cytoskeleton were stained with DAPI, anti-vinculin, and TRITC conjugated phalloidin following the same staining protocol as described above. Samples were fixed and permeabilized following the same procedure as defined previously. Samples were labeled with anti-vinculin (1:250 dilution in blocking solution) for one hour at RT, followed by labeling with TRITC conjugated phalloidin (1:500 dilution) and goat polyclonal secondary antibody to mouse IgG - H&L (FITC) (1:1000 dilution) (Abram®, Toronto, ON) for one hour. Scaffolds were labeled with DAPI at 0.5 μg/mL in PBS for 10 minutes and washed 3 times with blocking

solution between each step, and viewed using a confocal microscope. Images were analyzed using Image ProPremier software. Angles of the major axis of cell nuclei from 4–6 images were measured to quantify cell axis angle. Standard cell area was determined by dividing the total area of f-actin stain by the number of cell nuclei.

2.8. Gene Expression

Genes for matrix proteins and other ECM components were tested on day 7 from cells removed from each scaffold in triplicate. RNA extraction and cDNA synthesis was performed following published protocols[34]. Media was aspirated off the scaffolds, they were washed two times in PBS, and then 2 mL of trypsin/EDTA was added to the scaffold wells and incubated for 2 minutes. Fresh media was then added to each scaffold and the suspension was pipetted into a 15 mL Falcon tube. RNA was extracted using RNeasy Mini Kit (Qiagen, Toronto, ON) and its instructions. A NanoDrop™ 1000 (Human Mobility Research Center, Queen's University) was used to measure the RNA yield and purity.

Before qRT-PCR was performed RNA was reverse transcribed into cDNA using the Quantitect Reverse Transcription kit (Qiagen, Toronto, ON). Transcription was carried out in a ThermoCycler (HMRC, Queen's University) at 42°C for 15 min followed by 3 min at 95°C then immediately placed on ice or stored at −20°C. Before continuing with qRT-PCR, the cDNA was diluted in RNase free water for a final concentration of 2.5 ng/uL. qRT-PCR reaction was set up using Kapa SYBR Fast Roche LightCycler® Master Mix (Kapa Biosystems, Boston, MA). Genes of interest were collagen-1, collagen-3, fibronectin, fibromodulin, elastin, and decorin, with β-actin as a housekeeping gene. Primers were from Integrated DNA Technologies (Coralville, IA), and the sequences are listed below in Table 1. Triplicates of each cDNA sample were run, and DNA amounts for each replicate were 5 ng for β-actin, collagen-1, -3, and fibronectin, 10 ng for decorin, and 20 ng for elastin and fibromodulin. qRT-PCR was performed using a Roche LightCycler 480 with clear 96 well plates (Roche, Laval, QC). The program that was run was pre-incubation cycle for 3 minutes at 95°C, amplification for 40 cycles of; 10 seconds at 95°C, 20 seconds at 55°C, and 10 seconds at 72°C, then a melting curve with 5 seconds at 95°C, 1 minute at 65°C, and 10 seconds at 97°C, and finally a cooling phase for 1 minute at 40°C. Ct values were calculated using the second derivative maximum method on the LC 480 Roche analysis program, and Tm calling was performed to check for contamination. Fold expression analysis was done using the ΔΔCt method. To perform the relative gene quantification on the qRT-PCR data the $2^{-\Delta\Delta Ct}$ method was used. The reference, or housekeeping, gene used in this study was β-actin.

2.9. Statistics

Data are presented as the mean ± standard deviation. Comparisons for all data were considered significant at $p < 0.05$. Data collected from fiber diameter, pore size, ELP4 surface concentrations, and cell coverage area were compared using an independent student t-test. Mechanical testing, cell orientation, and cell proliferation data were compared with one-way ANOVA using a Bonferroni post hoc analysis. Finally, qRT-PCR data was compared using multiple independent student t-tests with Sidal-Bonferroni post-hoc analysis.

3. Results

3.1. Scaffold Characterization

To investigate the potential of aligned scaffolds in vocal fold constructs, aligned and unaligned polyurethane scaffolds were made and their morphological characteristics were determined. Unaligned and aligned scaffolds were prepared with minimal fiber fusion (Figure 1) using mandrel surface speeds of 5 cm/s and 410 cm/s and a 10% w/v solution. Randomly oriented fibers, as well as a highly aligned fiber orientation were confirmed. There was a very broad and equal distribution of fiber angles for the unaligned scaffolds, and aligned scaffolds have the majority of fibers oriented around 20° of the reference angle. The average absolute angles were determined for the scaffolds, and using this analysis a value of 45° represents completely random orientation while a value of 0° represents perfectly aligned orientation of fibers. There was a significant difference in the absolute angle between the unaligned scaffolds (43.3 ± 25.24°) and aligned scaffolds (17.0 ± 19.6°) ($p<0.0001$) (Figure 1). Scaffolds were further characterized by measuring the fiber diameters. Aligned and unaligned scaffolds have similar fiber diameter distributions with diameters ranging from 250 nm to 3.25 μm, indicating that the scaffolds consist of micro-sized fibers with a diameter range of 3 μm. Aligned scaffolds had significantly smaller average fiber diameter (1.2 ± 0.5 μm) compared to unaligned scaffolds (1.4 ± 0.6 μm) ($p<0.0001$) (Figure 1). There was no significant difference for average pore sizes between scaffold types ($p = 0.2629$). The average pore size for the aligned scaffolds was 9.25 ± 4.14 μm compared to unaligned 9.87 ± 5.9 μm

3.2. Mechanical Properties

Scaffolds were subjected to uniaxial tensile testing in the preferred and cross-preferred directions to determine initial modulus of elasticity. Representative stress-strain curves for the scaffolds are seen in Figure 2. The ultimate tensile stress was unable to be determined due to a maximum extension reached by the machine, however all three conditions reached close to 350% strain. Initial moduli for the aligned samples in the preferred and cross-preferred directions were 14.5 ± 1.3 and 0.32 ± 0.02 MPa, respectively. Moreover, the initial moduli for the unaligned samples in the preferred and cross-preferred directions were 4.6 ± 0.4 and 0.6 ± 0.06 MPa respectively.

3.3. Elastin Coating

Fastin™ Elastin assay was used as an indirect test for ELP4 adsorption. There was no significant difference found between the aligned (4.2 ± 0.9 $\mu g/cm^2$) and unaligned (3.9 ± 1.2 $\mu g/cm^2$) scaffolds specific to the amount of ELP4 adsorbed ($p=0.6221$).

3.4. HVFF Viability

Using Live/Dead® staining, alamarBlue® and PicoGreen® assays, HVFF viability was determined. On days 3 and 7 Live/Dead® stains were used on the scaffolds. There was a high confluence of cells on all scaffold types with minimal evidence of dead cells by day 7 (Figure 3). Dead cells present appear to be in small clusters due to the size of the red dots seen in the images being larger than a cell nucleus. Figure 4 illustrates alamarBlue®

fluorescence readings and PicoGreen® DNA amounts on the two scaffold alignments and coatings -- aligned fibronectin coated scaffolds (AFN), unaligned fibronectin coated scaffolds (UFN), aligned fibronectin and ELP4 coated scaffolds (AEP) and unaligned fibronectin and ELP4 coated scaffolds (UEP). Based upon alamarBlue® readings, cell cultures demonstrated increased metabolic activity over the 7 day period, and there was little difference between the cells on the different scaffold conditions at each time point. There were significant differences between day 1 to day 7 on AEP scaffolds ($p=0.011$), as well from day 1 to 7 ($p<0.0001$), and 3 to 7 ($p=0.005$) on UEP scaffolds. As well there was a difference on day 7, indicating more metabolically active cells on the UEP scaffold compared to the AEP ($p=0.015$) and UFN scaffolds ($p=0.004$). PicoGreen results further suggested increases in cell amounts. There were significant differences in DNA amounts between day 1 and day 7 readings for AEP ($p=0.002$), AFN ($p=0.010$), and UFN ($p=0.001$)), but not for UEP ($p=0.197$).

To further interpret these results alamarBlue® fluorescent readings and PicoGreen® DNA amounts for each scaffold condition were averaged and results were normalized against each other (Figure 4) Higher metabolic activity per cell was measured on day 1 and a reduction of metabolic activity per cell on days 3 and 7, with significant differences found in most groups ($p<0.0001$ for AFN and UFN, $p=0.011$ for AEP) except for UEP ($p=0.99$).

3.5. HVFF Morphology

Morphology of the HVFF on the scaffolds was investigated using immunostaining. None of the samples stained positive for α-SMA; scaffolds did not appear to promote myoblastic differentiation (Figure 5). Collagen-1 had deposited on the scaffolds by day 3, and is also apparent on day 7. Immunostaining for f-actin, and DAPI was completed on days 3 and 7 to more accurately characterize the morphology of the cells on the different scaffold architectures and coatings (Figure 6). HVFF on aligned scaffolds with and without ELP4 coating had average absolute angles of cell axis of 10.6 ± 14.6° and 8.2 ± 12.1° respectively, while on the unaligned scaffolds with and without ELP4 coating had absolute angles of 40.1 ± 21.8° and 63.0 ± 23.2° respectively. There was a statistical significance found between all conditions ($p<0.001$) except for between AFN and AEP ($p<0.1876$). The standard cell areas for AFN and AEP were 362.5 ± 87.3 μm^2/cell and 358.1 ± 132.9 μm^2/cell, respectively, and for UFN and UEP are 555.5 ± 129.0 μm^2/cell and 449.8 ± 174.1 μm^2/cell, respectively.

3.6. Gene Expression

Relative gene expression levels were tested between the aligned and unaligned, as well as between coated and non-coated samples on day 7 of culture (Figure 7). There were significant differences in the transcript expression of collagen-3 (COL3), and elastin (ELN). When using AEP as the treated sample, there was a significant increase, almost two-fold, in the elastin gene expression level compared to the AFN control sample ($p=0.0052$). When comparing between unaligned coated and non-coated, UEP also had significantly elevated elastin gene levels, though not to the same extent, compared to UFN ($p=0.0036$). Collagen-3 was significantly elevated in UEP compared to UFN ($p=0.002$). AEP had elevated elastin gene levels compared to UEP ($p=0.006$). There was no difference in gene expression for any of the genes between the aligned and unaligned non-coated samples ($p<0.05$).

4. Discussion

Topographical features of substrates used in tissue engineering applications have been shown to affect cell proliferation, differentiation, migration, orientation, and secretion of ECM[35]. Electrospun scaffolds are a promising option for tissue engineering as their architecture, topography, and mechanical properties can mimic that of native tissues[36]. Surface and bulk properties including pore size, fiber diameter, and fiber alignment can be easily altered by changing parameters during the electrospinning process, making the scaffolds tunable to most tissues[37]. Fiber alignment in the electrospun scaffolds, in particular, is an important property as many tissues in the body, including vocal folds, express aligned structures[11]. The present investigation focused on constructing an elastomeric electrospun scaffold to evaluate parameters important for the application of vocal fold lamina propria tissue constructs. These elastomeric scaffolds were used exclusively as in vitro constructs, to evaluate the use of ELP4 coatings and the effect of alignment on HVFF. Such model elastomeric scaffolds are useful for vocal fold tissue engineering to better understand how the cells interact with the scaffold, as well as how they respond to vibration on materials with different properties[34]. Viability, morphology, and ECM gene expression of HVFF grown on scaffolds with differing fiber alignment and elastin-like polypeptide coating were investigated. Elastin-like polypeptides have been examined as coatings on biomaterials for several vascular applications due to their ability to reduce platelet adhesion and activation, and make the surface less thrombogenic[22, 23]. The coatings have also promoted cell attachment in endothelial cells, and may do the same with fibroblast cells as they have a surface receptor for the elastin binding motif VGVAPG[24]. As elastin, and its organization in the ECM, plays a key role in the function of the vocal folds, promoting deposition during wound healing may improve biological function[16].

Tecoflex® was successfully electrospun into two different scaffolds; one with highly aligned fibers, and another with randomly aligned networks. The mandrel rotation speeds used in this work proved effective in creating randomly deposited fibers, as well as aligned fibrous networks without apparent defects or breakage of the fibers. Research on cell response to different fiber diameters indicates that the diameter difference seen in this work should not have a significant effect on cell fate processes[38–41]. In addition, pore sizes in the aligned and unaligned scaffolds were not statistically different, thereby providing similar surface area for cell contact on each scaffold type. For both scaffold types, pore diameters ranged from roughly 5–20 μm. Though both the aligned and unaligned scaffolds had several pores at all sizes within this range, the majority of pores were under 10 μm in diameter. Finally, human dermal fibroblasts had higher elastin gene expression on fiber diameters ranging from 0.6 – 1.2 μm, similar to the one in this work, compared to larger and smaller diameters tested[41].

Aligned and unaligned electrospun Tecoflex has mechanical characteristics typical of other electrospun scaffolds when subjected to stress-strain testing. Namely, as fiber orientation increases the material becomes stiffer in the preferred direction, and more elastic in the cross-preferred direction[37, 42, 43]. The aligned scaffold had similar properties to that of human vocal fold lamina propria, with a high initial elastic modulus when pulled in the preferred direction, and much lower modulus in the cross-preferred direction[43, 44]. It

should be noted that despite the scaffold anisotropy, the uniaxial tensile properties of the scaffolds were an order of magnitude greater than that previously reported for the vocal fold lamina propria[3, 19]. For future investigations, a biodegradable scaffold material would need to be used whose material properties better match human vocal fold tissue. One method could be to co-spin biodegradable polyurethane with ELP4 to provide higher elasticity in the preferred direction, while reducing the initial elastic modulus[43].

HVFF seeded onto scaffolds remained viable over a 7 and 14 day period. All scaffold conditions showed cell proliferation, with scaffolds on day 7 having a high degree of confluence demonstrating that the scaffolds are capable of sustaining a viable cell population without the development of a myofibroblast phenotype. Many groups have demonstrated that fiber alignment has an effect on the growth of different types of cells, such as fibroblasts and smooth muscle cells, and aligned fibers improves the alignment of the cells[12, 14, 42]. We confirmed that HVFFs orient along aligned fibers as well, while showing no sense of orientation on the random fibers.

Tissue engineering scaffolds that present a combination of fibrous substrate and ELP4 coating could be considered structurally and functionally biomimetic. Our findings support that specific scaffold architecture combined with ELP4 coating promoted elastin gene expression. UEP and AEP scaffolds had significantly higher elastin expression compared to UFN and AFP scaffolds and AEP had higher elastin transcription levels than UEP. During development, cells such as fibroblasts, smooth muscle cells, and endothelial cells synthesize elastin[45], which must be able to withstand high stress and relaxation cycles over the course of the organism’s lifespan. Elastin in scarred animal vocal folds is unorganized and less dense two months post injury[19, 46]; human vocal folds have been characterized by disorganized elastin, or complete lack of elastin when scarred[47]. The capacity to fabricate new, organized elastin has major implications in restoring proper function to the vocal fold tissue after injury and scarring. Both elastin and ELP4 lack the mechanical integrity to undergo scaffold formation by electrospinning, and as such, must be adsorbed on top of another scaffold material or electrospun with another material. The lack of differences in collagen or other ECM gene expression in response to topography or ELP4 coating in this investigation does not correspond to previous findings where aligned fibers induced collagen production compared to unaligned[48]. Our findings suggesting that HVFF, while receptive to topographic cues from electrospun scaffolds affecting cell behavior and fate, may respond differently than fibroblasts from other parts of the body. Further investigation is warranted with cellular therapy candidates for the vocal fold lamina propria, including adult mesenchymal stem cells and induced pluripotent stem cells.

Taken together, our data support that aligned electrospun scaffolds with an ELP coating could provide optimum culturing conditions for vocal fold tissue engineering applications. ELP4 coating promoted elastin gene expression regardless of topography, with the aligned nanofibers producing significantly greatest transcript levels. All scaffolds promoted viability and proliferation of HVFF, but scaffold topography affected the orientation of the cells. Aligned fibers produced arranged, confluent cell layers whereas unaligned nanofibers resulted in disorganized cell layers. Using oriented electrospun ELP coated fibers could provide significant advantages for guided vocal fold lamina propria reconstruction.

Acknowledgments

We would like to thank Xia Chen, PhD, University of Wisconsin Madison for technical assistance. NIH NIDCD R01 4336 and the Natural Sciences and Engineering Research Council of Canada and Queen's University supported this work.

References

1. Ramig LO, Verdolini K. Treatment efficacy: Voice disorders. J Speech Lang Hear Res. 1998; 41:S101–S116. [PubMed: 9493749]
2. Branski RC, Verdolini K, Sandulache V, Rosen CA, Hebda PA. Vocal fold wound healing: A review for clinicians. J Voice. 2006; 20:432–442. [PubMed: 16324825]
3. Kutty JK, Webb K. Tissue engineering therapies for the vocal fold lamina propria. Tissue Eng Part B Rev. 2009; 15:249–262. [PubMed: 19338432]
4. Hirano S. Current treatment of vocal fold scarring. Curr Opin Otolaryngol Head Neck Surg. 2005; 13:143–147. [PubMed: 15908810]
5. Hirano S, Bless DA, Nagai H, Rousseau B, Welham NV, Montequin DW, Ford CN. Growth factor therapy for vocal fold scarring in a canine model. Ann Otol Rhinol Laryngol. 2004; 113:777–785. [PubMed: 15535139]
6. Hirano S, Bless DM, Rousseau B, Welham N, Montequin D, Chan RW, Ford CN. Prevention of vocal fold scarring by topical injection of hepatocyte growth factor in a rabbit model. Laryngoscope. 2004; 114:548–556. [PubMed: 15091233]
7. Chhetri DK, Head C, Revazova E, Hart S, Bhuta S, Berke GS. Lamina propria replacement therapy with cultured autologous fibroblasts for vocal fold scars. Otolaryngol Head Neck Surg. 2004; 131:864–870. [PubMed: 15577782]
8. Cedervall J, Ahrlund-Richter L, Svensson B, Forsgren K, Maurer FHJ, Vidovska D, Hertegard S. Injection of embryonic stem cells into scarred rabbit vocal folds enhances healing and improves viscoelasticity: Short-term results. Laryngoscope. 2007; 117:2075–2081. [PubMed: 17895858]
9. Kanemaru SI, Nakamura T, Omori K, Kojima H, Magrufov A, Hiratsuka Y, Hirano S, Ito J, Shimizu Y. Regeneration of the vocal fold using autologous mesenchymal stem cells. Ann Otol Rhinol Laryngol. 2003; 112:915–920. [PubMed: 14653358]
10. Murugan R, Ramakrishna S. Design strategies of tissue engineering scaffolds with controlled fiber orientation. Tissue Eng. 2007; 13:1845–1866. [PubMed: 17518727]
11. Parrag IC, Zandstra PW, Woodhouse KA. Fiber alignment and coculture with fibroblasts improves the differentiated phenotype of murine embryonic stem cell-derived cardiomyocytes for cardiac tissue engineering. Biotechnol Bioeng. 2012; 109:813–822. [PubMed: 22006660]
12. Zhong SP, Teo WE, Zhu X, Beuerman RW, Ramakrishna S, Yung LYL. An aligned nanofibrous collagen scaffold by electrospinning and its effects on in vitro fibroblast culture. J Biomed Mater Res A. 2006; 79A:456–463. [PubMed: 16752400]
13. Chew SY, Mi R, Hoke A, Leong KW. The effect of the alignment of electrospun fibrous scaffolds on Schwann cell maturation. Biomaterials. 2008; 29:653–661. [PubMed: 17983651]
14. Xu CY, Inai R, Kotaki M, Ramakrishna S. Aligned biodegradable nanotibrous structure: A potential scaffold for blood vessel engineering. Biomaterials. 2004; 25:877–886. [PubMed: 14609676]
15. Gray SD, Titze IR, Alipour F, Hammond TH. Biomechanical and histologic observations of vocal fold fibrous proteins. Annals of Otology Rhinology and Laryngology. 2000; 109:77–85.
16. Moore J, Thibeault S. Insights into the role of elastin in vocal fold health and disease. J Voice. 2012; 26:269–275. [PubMed: 21708449]
17. Debelle L, Tamburro AM. Elastin: Molecular description and function. Int J Biochem Cell Biol. 1999; 31:261–272. [PubMed: 10216959]
18. Rousseau B, Hirano S, Scheidt TD, Welham NV, Thibeault SL, Chan RW, Bless DM. Characterization of vocal fold scarring in a canine model. Laryngoscope. 2003; 113:620–627. [PubMed: 12671417]

19. Thibeault SL, Gray SD, Bless DM, Chan RW, Ford CN. Histologic and rheologic characterization of vocal fold scarring. J Voice. 2002; 16:96–104. [PubMed: 12002893]
20. Osborne JL, Farmer R, Woodhouse KA. Self-assembled elastin-like polypeptide particles. Acta Biomater. 2008; 4:49–57. [PubMed: 17881311]
21. Bellingham CM, Lillie MA, Gosline JM, Wright GM, Starcher BC, Bailey AJ, Woodhouse KA, Keeley FW. Recombinant human elastin polypeptides self-assemble into biomaterials with elastin-like properties. Biopolymers. 2003; 70:445–455. [PubMed: 14648756]
22. Srokowski EM, Blit PH, McClung WG, Brash JL, Santerre JP, Woodhouse KA. Platelet adhesion and fibrinogen accretion on a family of elastin-like polypeptides. J Biomater Sci Polym Ed. 2011; 22:41–57.
23. Woodhouse KA, Klement P, Chen V, Gorbet MB, Keeley FW, Stahl R, Fromstein JD, Bellingham CM. Investigation of recombinant human elastin polypeptides as non-thrombogenic coatings. Biomaterials. 2004; 25:4543–4553. [PubMed: 15120499]
24. Sales VL, Engelmayr GC Jr, Johnson JA Jr, Gao J, Wang Y, Sacks MS, Mayer JE Jr. Protein precoating of elastomeric tissue-engineering scaffolds increased cellularity, enhanced extracellular matrix protein production, and differentially regulated the phenotypes of circulating endothelial progenitor cells. Circulation. 2007; 116:I55–63. [PubMed: 17846326]
25. Kamoun A, Landeau JM, Godeau G, Wallach J, Duchesnay A, Pellat B, Hornebeck W. Growth stimulation of human skin fibroblasts by elastin-derived peptides. Cell Adhes Commun. 1995; 3:273–281. [PubMed: 8821030]
26. Brassart B, Randoux A, Hornebeck W, Emonard H. Regulation of matrix metalloproteinase-2 (gelatinase a, mmp-2), membrane-type matrix matelloproteinase-1 (mt1-mmp) and tissue inhibitor of metalloproteinases-2 (timp-2) expression by elastin-derived peptides in human ht-1080 fibrosarcoma cell line. Clin Exp Metastasis. 1998; 16:489–500. [PubMed: 9872597]
27. Surrao DC, Waldman SD, Amsden BG. Biomimetic poly(lactide) based fibrous scaffolds for ligament tissue engineering. Acta Biomater. 2012; 8:3996.7–400.
28. Chen X, Thibeault SL. Novel isolation and biochemical characterization of immortalized fibroblasts for tissue engineering vocal fold lamina propria. Tissue Eng Part C Methods. 2009; 15:201–212. [PubMed: 19108681]
29. Srokowski EM, Woodhouse KA. Surface and adsorption characteristics of three elastin-like polypeptide coatings with varying sequence lengths. Journal of Materials Science-Materials in Medicine. 2013; 24:71–84. [PubMed: 23053802]
30. Chen X, Thibeault SL. Response of Fibroblasts to Transforming Growth Factor-beta 1 on Two-Dimensional and in Three-Dimensional Hyaluronan Hydrogels. Tissue Engineering Part A. 2012; 18:2528–38. [PubMed: 22734649]
31. Jette ME, Hayer SD, Thibeault SL. Characterization of human vocal fold fibroblasts derived from chronic scar. Laryngoscope. 2013; 123:738–45. [PubMed: 23444190]
32. Johnson BQ, Fox R, Chen X, Thibeault S. Tissue Regeneration of the Vocal Fold Using Bone Marrow Mesenchymal Stem Cells and Synthetic Extracellular Matrix Injections in Rats. Laryngoscope. 2010; 120:537–45. [PubMed: 20131370]
33. Vyas B, Ishikawa K, Duflo S, Chen X, Thibeault SL. Inhibitory Effects of Hepatocyte Growth Factor and Interleukin-6 on Transforming Growth Factor-beta 1 Mediated Vocal Fold Fibroblast-Myofibroblast Differentiation. Annals of Otology Rhinology and Laryngology. 2010; 119:350–7.
34. Gaston J, Rios BQ, Bartlett R, Berchtold C, Thibeault SL. The response of vocal fold fibroblasts and mesenchymal stromal cells to vibration. PLoS One. 2012:7.
35. Flemming RG, Murphy CJ, Abrams GA, Goodman SL, Nealey PF. Effects of synthetic micro- and nano-structured surfaces on cell behavior. Biomaterials. 1999; 20:573–588. [PubMed: 10213360]
36. Li WJ, Laurencin CT, Caterson EJ, Tuan RS, Ko FK. Electrospun nanofibrous structure: A novel scaffold for tissue engineering. J Biomed Mater Res. 2002; 60:613–621. [PubMed: 11948520]
37. Courtney T, Sacks MS, Stankus J, Guan J, Wagner WR. Design and analysis of tissue engineering scaffolds that mimic soft tissue mechanical anisotropy. Biomaterials. 2006; 27:3631–3638. [PubMed: 16545867]

38. Kim KW, Lee KH, Khil MS, Ho YS, Kim HY. The effect of molecular weight and the linear velocity of drum surface on the properties of electrospun poly(ethylene terephthalate) nonwovens. Fiber Polym. 2004; 5:122–127.
39. Badami AS, Kreke MR, Thompson MS, Riffle JS, Goldstein AS. Effect of fiber diameter on spreading, proliferation, and differentiation of osteoblastic cells on electrospun poly(lactic acid) substrates. Biomaterials. 2006; 27:596–606. [PubMed: 16023716]
40. Bashur CA, Dahlgren LA, Goldstein AS. Effect of fiber diameter and orientation on fibroblast morphology and proliferation on electrospun poly(d, l-lactic-co-glycolic acid) meshes. Biomaterials. 2006; 27:5681–5688. [PubMed: 16914196]
41. Bashur CA, Shaffer RD, Dahlgren LA, Guelcher SA, Goldstein AS. Effect of fiber diameter and alignment of electrospun polyurethane meshes on mesenchymal progenitor cells. Tissue Eng Part A. 2009; 15:2435–2445. [PubMed: 19292650]
42. Matthews JA, Wnek GE, Simpson DG, Bowlin GL. Electrospinning of collagen nanofibers. Biomacromolecules. 2002; 3:232–238. [PubMed: 11888306]
43. Parrag IC, Woodhouse KA. Development of biodegradable polyurethane scaffolds using amino acid and dipeptide-based chain extenders for soft tissue engineering. J Biomater Sci Polym Ed. 2010; 21:843–862. [PubMed: 20482988]
44. Kumbar SG, Nukavarapu SP, James R, Nair LS, Laurencin CT. Electrospun poly(lactic acid-co-glycolic acid) scaffolds for skin tissue engineering. Biomaterials. 2008; 29:4100–4107. [PubMed: 18639927]
45. Alipour F, Vigmostad S. Measurement of vocal folds elastic properties for continuum modeling. J Voice. 2012; 26:9.
46. Rousseau B, Hirano S, Chan RW, Welham NV, Thibeault SL, Ford CN, Bless DM. Characterization of chronic vocal fold scarring in a rabbit model. J Voice. 2004; 18:116–124. [PubMed: 15070231]
47. Chan RW, Titze IR. Viscoelastic shear properties of human vocal fold mucosa: Measurement methodology and empirical results. J Acoust Soc Am. 1999; 106:2008–2021. [PubMed: 10530024]
48. Lee CH, Shin HJ, Cho IH, Kang YM, Kim IA, Park KD, Shin JW. Nanofiber alignment and direction of mechanical strain affect the ECM production of human ACL fibroblast. Biomaterials. 2005; 26:1261–1270. [PubMed: 15475056]

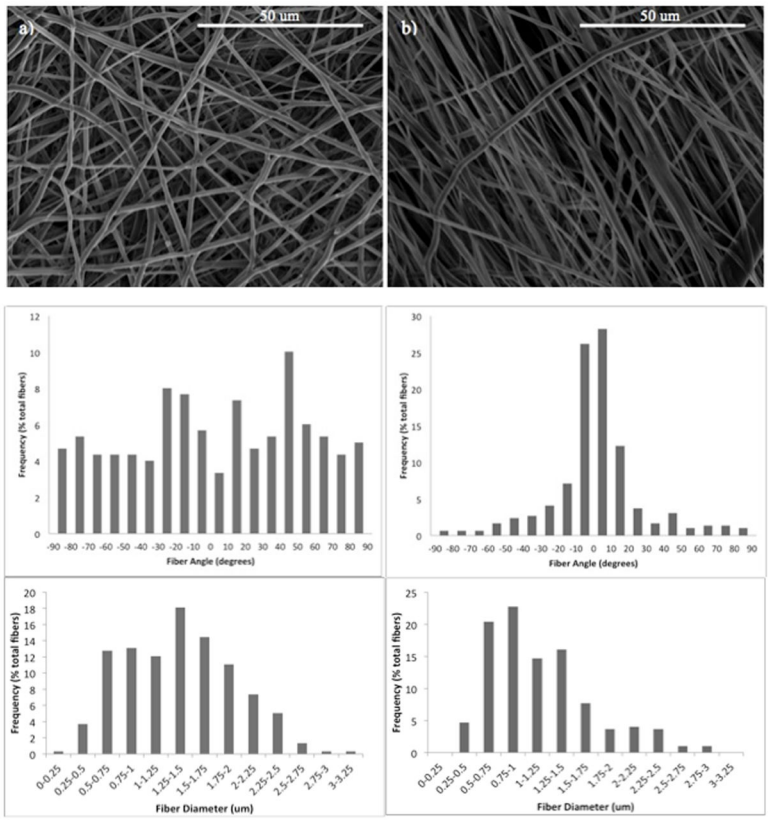

Figure 1.

SEM image of a) unaligned scaffold, b) aligned scaffold. Fiber angle quantification. c) unaligned scaffold with a uniform distribution, d) aligned scaffold oriented around 20 of the reference angle. Fiber diameter distribution. e) unaligned scaffold, f) aligned scaffold.

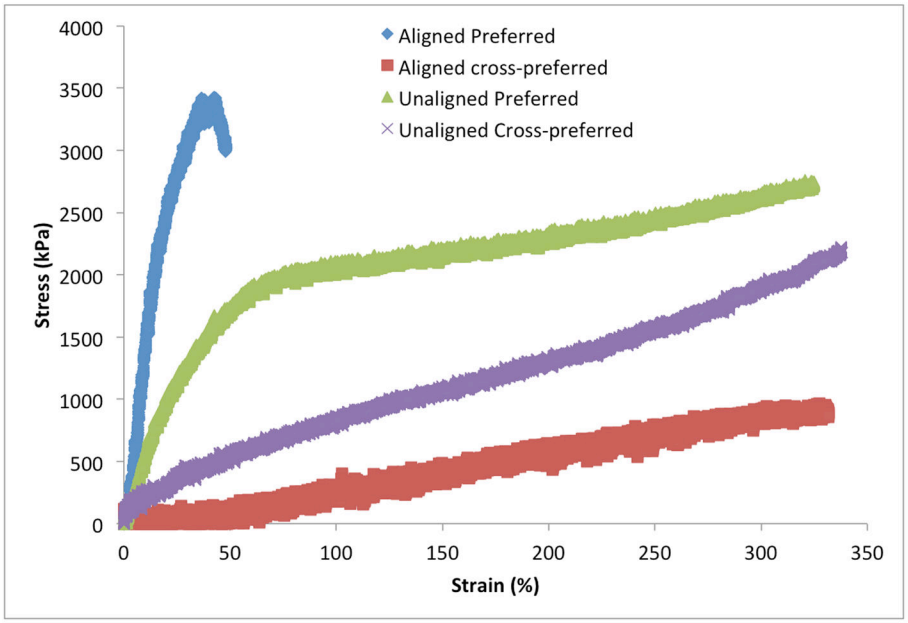

Figure 2.
Stress-Strain curves of the aligned and unaligned scaffolds

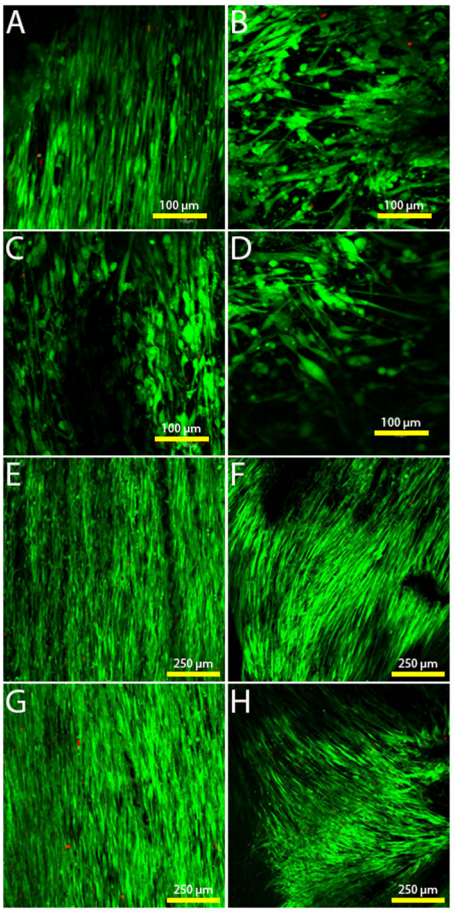

Figure 3.

Live/dead staining of the cells on the different scaffold types. Green = viable cells, red = dead cells. A) Aligned scaffold with fibronectin coating on day 3. B) Unaligned scaffold with fibronectin coating on day 3. C) Aligned scaffold with ELP4 coating on day 3. D) Unaligned scaffold with ELP4 coating on day 3. E) Aligned scaffold with fibronectin coating on day 7. F) Unaligned scaffold with fibronectin coating on day 7. G) Aligned scaffold with ELP4 coating on day 7. H) Unaligned scaffold with ELP4 coating on day 7.

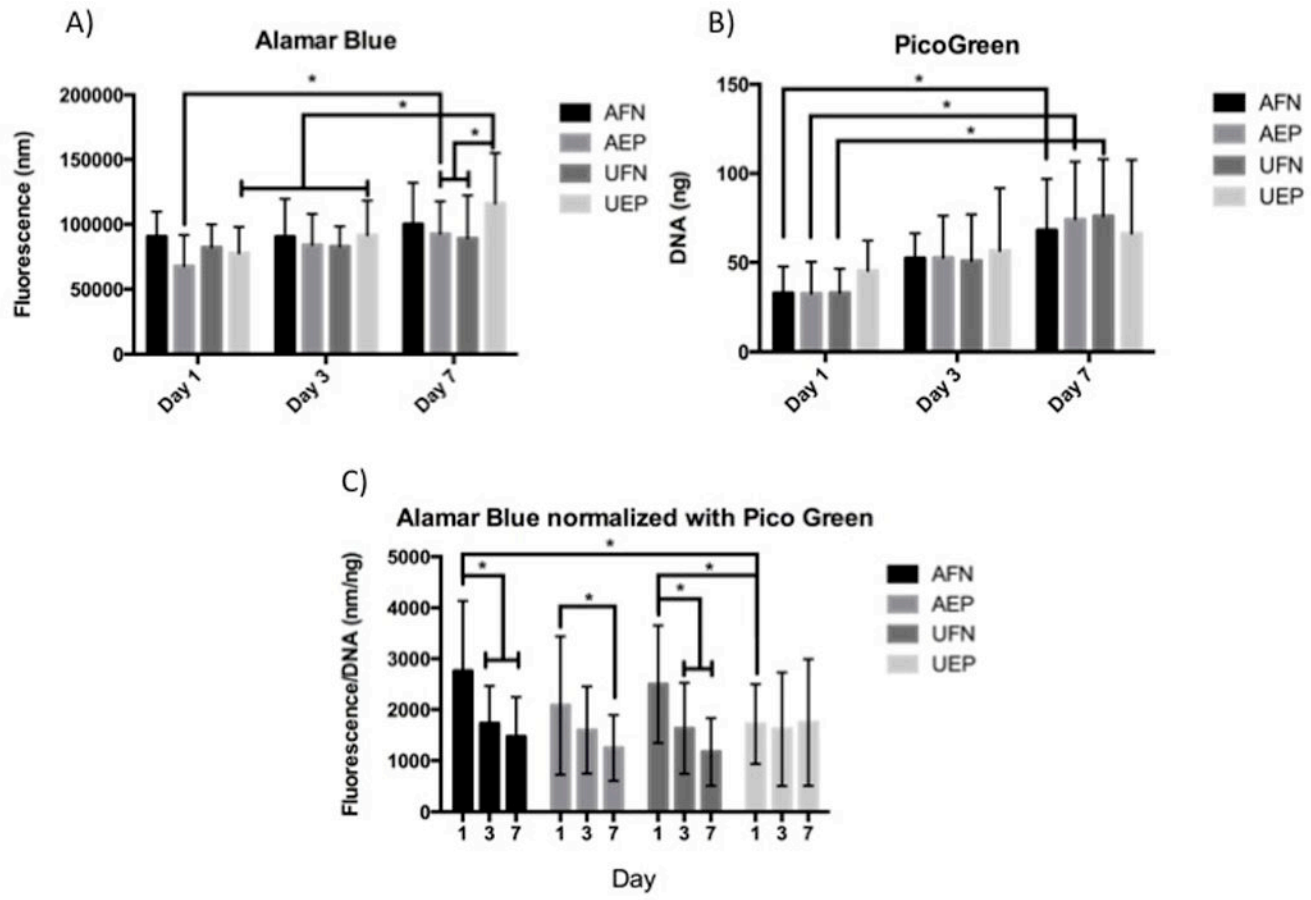

Figure 4.

A. alamarBlue® results of the cell seeded constructs over a 7 day period. AFN and UFN represent aligned and unaligned scaffolds with fibronectin coating, and AEP and UEP represent aligned and unaligned scaffolds coated in fibronectin and ELP4. **B**. PicoGreen® results of the cell seeded constructs over a 7 day period. AFN and UFN represent aligned and unaligned scaffolds with fibronectin coating, and AEP and UEP represent aligned and unaligned scaffolds coated in fibronectin and ELP4. **C**. alamarBlue® results normalized with PicoGreen® results or each scaffold type on days 1, 3 and 7. AFN and UFN represent aligned and unaligned scaffolds with fibronectin coating, and AEP and UEP represent aligned and unaligned scaffolds coated in fibronectin and ELP4. * indicates significance at $p < 0.05$

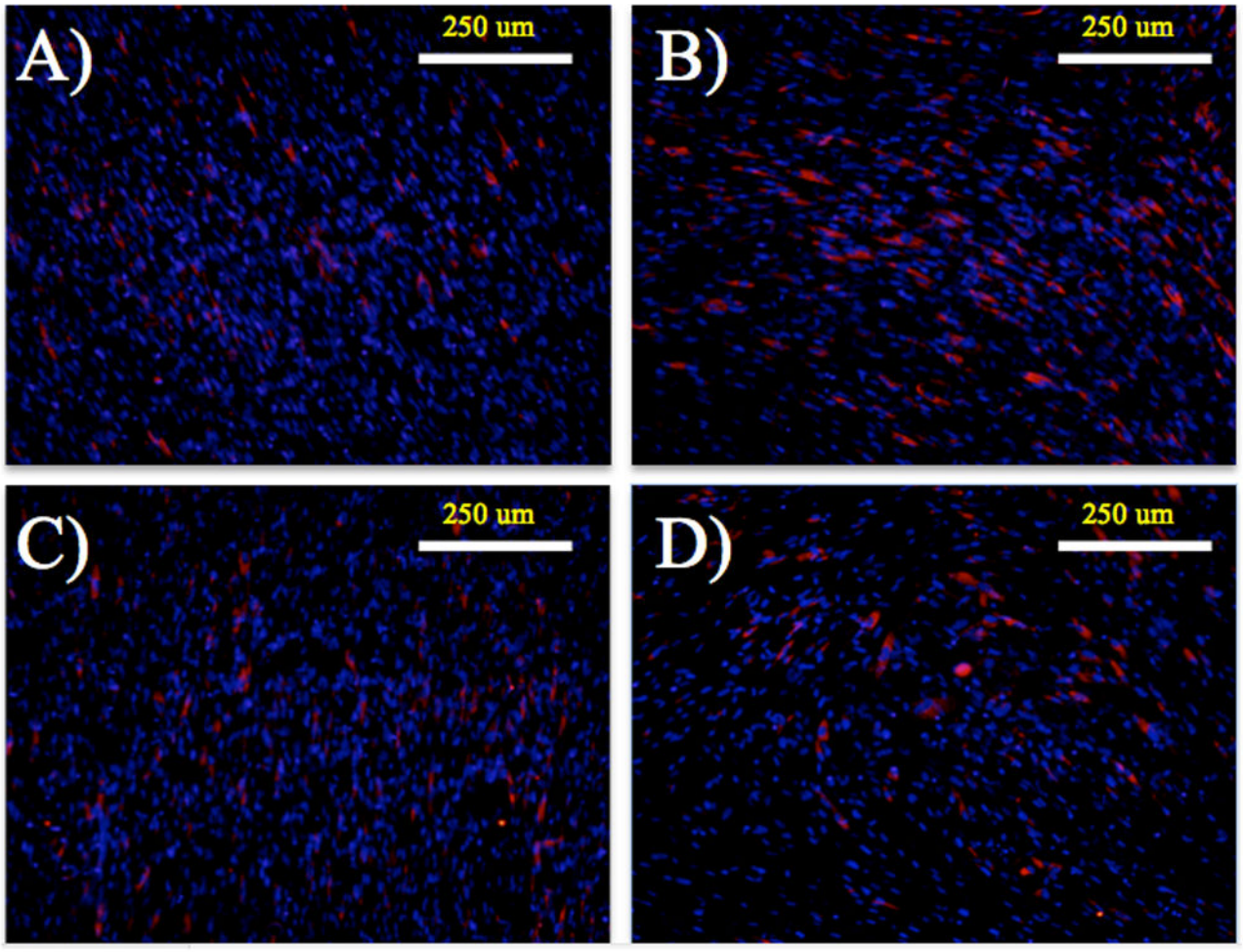

Figure 5.

HVFF seeded scaffolds stained for collagen-1 (red), α-SMA (green), and cell nuclei (blue) on day 7. A) Aligned scaffold with fibronectin coating. B) Unaligned scaffold with fibronectin coating. C) Aligned scaffold with ELP4 coating. D) Unaligned scaffold with ELP4 coating.

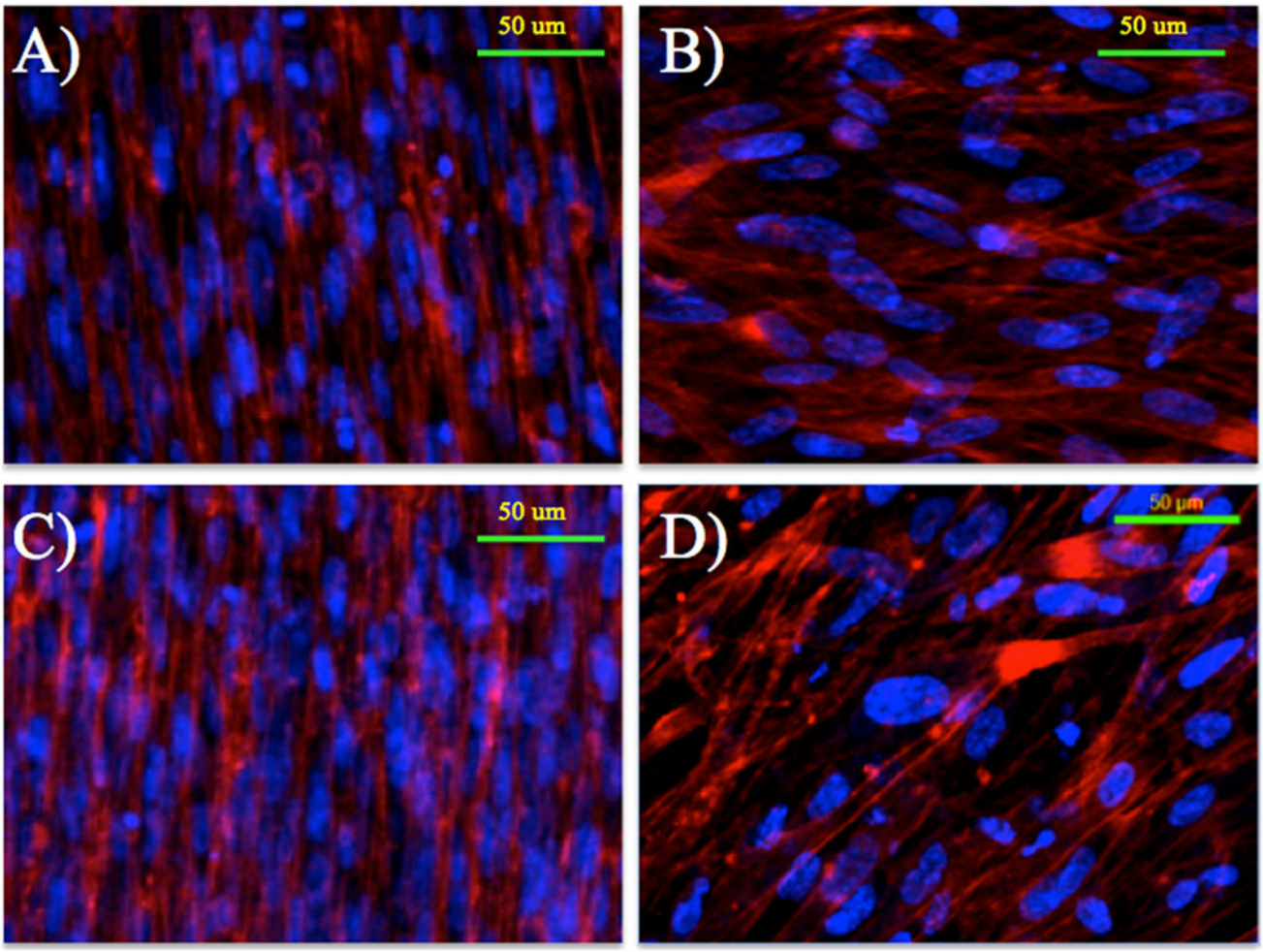

Figure 6.

Immunostained images of the seeded scaffolds on day 7. F-actin is stained red (TRITC) and the cell nuclei are blue (DAPI). A) Aligned scaffold with fibronectin coating. B) Unaligned scaffold with fibronectin coating. C) Aligned scaffold with ELP4 coating. D) Unaligned scaffold with ELP4 coating.

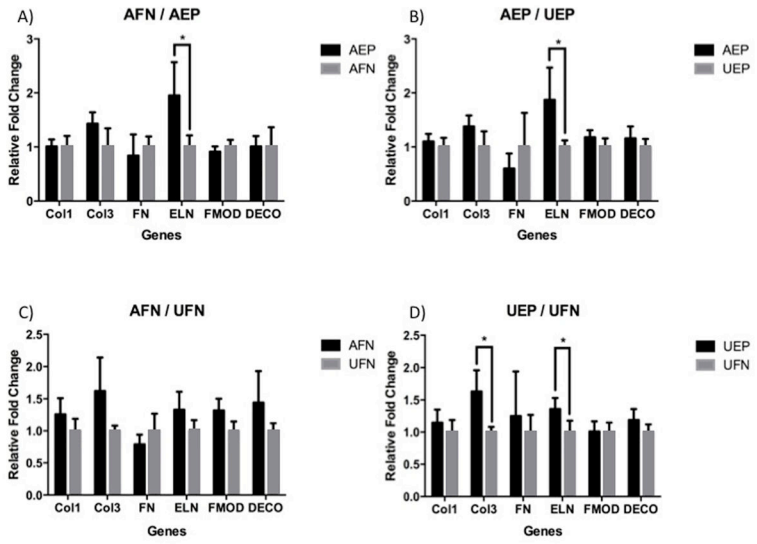

Figure 7.

A. Relative fold changes of target gene expression levels between aligned with ELP4 coating (AEP) and aligned with fibronectin coating (AFN). **B.** Relative fold changes of target gene expression levels between aligned with ELP4 coating (AEP) and unaligned with ELP4 coating (UEP). **C.** Relative fold changes of target gene expression levels between aligned with fibronectin coating (AFN) and unaligned with fibronectin coating (UFN). **D.** Relative fold changes of target gene expression levels between unaligned with ELP4 coating (UEP) and unaligned with fibronectin coating (UFN). * indicates significance at $p < .05$

Table 1

Primer Sequences

Primer Name	Primer Sequence
b-Actin	Forward - 5′-ACGTTGCTATCCAGGCTGTGCTAT-3′
	Reverse - 5′-CTCGGTGAGGATCTTCATGAGGTAGT-3′
Elastin	Forward - 5′-AAGCAGCAGCAAAGTTCGGT-3′
	Reverse - 5′-ACTAAGCCTGCAGCAGCTCCATA-3′
Fibromodulin	Forward - 5′-ATCCTGCTGGACCTGAGCTA-3′
	Reverse - 5′-GCAGCTGGTTGTAGGAGAGG-3′
Fibronectin	Forward - 5′-ACCTACGGATGACTCGTGCTTTGA-3′
	Reverse - 5′-CAAAGCCTAAGCACTGGCACAACA-3′
Collagen-1	Forward - 5′-AACAAATAAGCCATCACGCCTGCC-3′
	Reverse - 5′-TGAAACAGACTGGGCCAATGTCCA- 3′
Collagen-3	Forward - 5′-CCATTGCTGGGATTGGAGGTGAAA-3′
	Reverse - 5′-TTCAGGTCTCTGCAGTTTCTAGCGG- 3′
Decorin	Forward - 5′-GATGCAGCTAGCCTGAAAGG -3′
	Reverse - 5′-TCACACCCGAATAAGAAGCC-3′